Scripta Materialia 192 (2021) 89–93

Contents lists available at ScienceDirect

Scripta Materialia

journal homepage: www.elsevier.com/locate/scriptamat

# Can two-dimensional confinement trigger the fragile-to-strong crossover in phase-change supercooled liquids

Qian Zhang[a], Yimin Chen[a,b,*], Wenhao Leng[a], Jierong Gu[a], Yuanen Mao[a], Xiang Shen[a,*], Rongping Wang[a], Tiefeng Xu[a], Jun-Qiang Wang[c,*], Guoxiang Wang[a]

[a] Laboratory of Infrared Material and Devices & Key Laboratory of Photoelectric Materials and Devices of Zhejiang Province, Advanced Technology Research Institute, Ningbo University, Ningbo, 315211, China
[b] Department of Microelectronic Science and Engineering, School of Physical Science and Technology, Ningbo University, Ningbo, 315211, China
[c] CAS Key Laboratory of Magnetic Materials and Devices & Zhejiang Province Key Laboratory of Magnetic Materials and Application Technology, Ningbo Institute of Materials Technology & Engineering, Chinese Academy of Sciences, Ningbo, 315201, China

ARTICLE INFO

*Article history:*
Received 7 August 2020
Revised 7 October 2020
Accepted 8 October 2020

*Keywords:*
GeTe phase-change material
two-dimensional confinement
crystallization kinetics
fragile-to-strong crossover

ABSTRACT

Recent fragile-to-strong crossover (FSC) concept in the crystallization kinetics study of phase-change supercooled liquids (PCLs) is attractive for screening the high-performance phase-change materials. It is important to search the FSC behavior in confined PCLs, like the two-dimensional confined PCLs, which is believed has fast crystallization and good thermal stability. Together with the ultrafast differential scanning calorimetry measurement and the generalized Mauro-Yue-Ellison-Gupta-Allan viscosity model, we here studied the crystallization kinetics of two-dimensional confined GeTe PCLs. It was found such confined PCLs has distinct FSC with large crossover magnitude is 2, confirming two-dimensional confinement can trigger the FSC behavior in PCLs.



In past decades, the global demand for data storage and processing has grown exponentially. To meet this demand, research works have been devoted to the development of non-volatile memory [1]. Chalcogenide phase-change memory has received widespread attention as the most promising candidates for next-generation non-volatile memory, because of the excellent storage density, fast read and write speeds, strong data retention capabilities, low power consumption [2]. The data information storage is depended on the huge difference in electrical resistance and/or optical reflectivity between reversible crystalline and amorphous phase-change materials [3].

The researchers focused on the acceleration of crystallization speed and enhancement of thermal stability, which are the contradiction, in many years. Thus, a concept of fragile-to-strong crossover (FSC) was recently carried out in the phase-change supercooled liquids (PCLs) to solve above contradiction [4]. An ideal PCLs is expected to has distinct FSC behavior with fast crystallization speed close to melting temperature ($T_m$) that makes the switching speed faster, and low crystallization speed near to glass transition temperature ($T_g$) that increases the data retention capabilities [5]. It was reported the phase-change films (three-dimension), like $Ag_{5.5}In_{6.5}Sb_{59}Te_{29}$ [4] and $Zn_{28}Sb_{54}Te_{18}$ [5], have distinct FSC behavior in their PCLs. However, there is no any FSC behaviors was found in the conventional PCLs, like the GST [6] and GeTe [7]. Interestingly, the distinct FSC behavior was observed in confined nanoparticles (zero-dimension) GST [8] and GeTe [9]. It was found water has FSC behavior in many years ago [10], and afterwards the researchers claimed that such FSC would be enhanced in confined water [11]. Does this mean the structure confinement could enhance (or trigger) the FSC behavior in supercooled liquids?

Previous studies have confirmed the FSC behavior presents in GST and GeTe nanoparticles, but it is insufficient to support above assumption. In this work, we performed a two-dimension confined GeTe PCLs in $[GeTe(7nm)/W(6nm)]_{20}$ multi-layer film, and together with the ultrafast differential scanning calorimetry (FDSC) and the generalized Mauro-Yue-Ellison-Gupta-Allan (g-MYEGA) viscosity model to study its crystallization kinetics, and confirm whether structure confinement could trigger the FSC behavior in supercooled liquids.

The multi-layer films were deposited on the substrates of $SiO_2$/Si (100) and NaCl (100) by the magnetron co-sputtering method using separated GeTe alloy target and tungsten (W) metal target. GeTe and W were grown alternately with nano-scale thickness of 7 and 6 nm, respectively, which were *in situ* controlled by sputtering time and *ex situ* checked by scanning electron microscope (SEM, Thermo scientific, Verios G4 UC), to form

* Corresponding authors.
*E-mail addresses:* chenyimin@nbu.edu.cn (Y. Chen), shenxiang@nbu.edu.cn (X. Shen), jqwang@nimte.ac.cn (J.-Q. Wang).

https://doi.org/10.1016/j.scriptamat.2020.10.017
1359-6462/

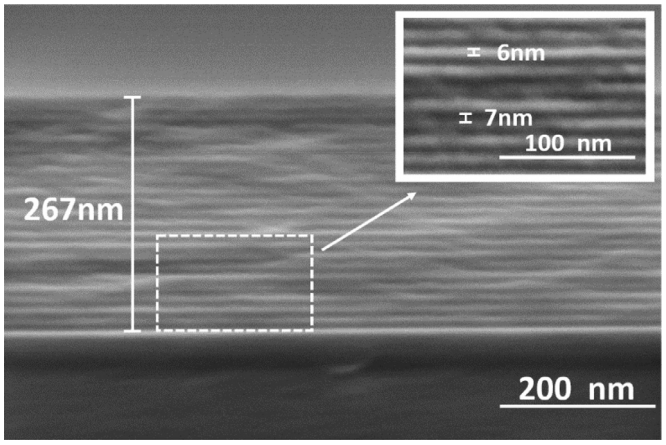


**Fig. 1.** Cross-sectional view of $[GeTe(7nm)/W(6nm)]_{20}$ film. The dark and bright layer indicate the GeTe and W ultra-thin film with thickness of 7 and 6 nm, respectively. The period number is 20, and the total thickness of the confined film is 267 nm (extra 7 nm comes from the last deposited GeTe layer).

$[GeTe(7nm)/W(6nm)]_{20}$ nano-scale multi-layer films. See the cross-sectional view of this confined film in Fig. 1. The DC power for GeTe target was set to 30 W and the RF power for W target was set to 40 W. The base and working pressures were set to $8 \times 10^{-6}$ and 3 mT, respectively. It should be noted that, we chose metal W as non-phase-change layer to confine the GeTe phase-change layer in this work, and then formed a two-dimension confined GeTe.

The NaCl (100) substrate used here is convenient to remove the films for FDSC measurements, and the films can be separated completely and very easily from the NaCl (100) substrate in distilled water just for 5 seconds. Loaded a separated flake on the USF-1 chip sensor and measured by FDSC (Mettler-Toledo Flash DSC 1) in a Ar atmosphere. Temperature calibration has been performed with In flake before the FDSC measurements. The measurement temperature range of this FDSC is -90 to 450 °C, the scanning rate range is 10 to 40000 K $s^{-1}$ for heating and 10 to 10000 K $s^{-1}$ for cooling, respectively. The sample size should be less than 200 × 200 $\mu$m with suitable thickness to avoid thermal lag. Such potential thermal lag in the FDSC measurement has been evaluated by using the Biot number. As we reported that, the Biot number of GeTe films with thickness of 1400 nm, is lower than 0.1 [7]. Thus, the Biot number of two-dimension confined $[GeTe(7nm)/W(6nm)]_{20}$ used here must be much lower than 0.1, because of the thinner total film thickness (267 nm) and larger thermal conductivity of W (160 W $m^{-1}$ $K^{-1}$). It implies the thermal lag between sample and heater surface can be negligible.

Fig. 2(a) shows the FDSC traces of $[GeTe(7nm)/W(6nm)]_{20}$ film with heating rate from 10 to 40000 K $s^{-1}$. An obvious exothermic peak can be found in each trace, which is caused by the crystallization. The corresponding peak temperature ($T_p$) is crystallization temperature, which increases from 514 to 576 K as the heating rate increases from 10 to 40000 K $s^{-1}$. More than four times measurement were performed at each heating rate in order to decrease the test error.

The $T_p$ values obtained from these FDSC traces are plotted by the Kissinger method, which can be expressed as [12],

$$\ln\left(\phi/T_p^2\right) = -Q/RT_p + A \quad (1)$$

where $Q$ is the activation energy for crystallization, $R$ is the gas constant (8.314 J $mol^{-1}$ $K^{-1}$, and $A$ is a constant. As shown in Fig. 2(b), thanks to the intact two-dimension confined film, which gets from the NaCl substrate used here, we obtained more convergent $T_p$ data compared to that from GeTe film (gray data). Apparently, the Kissinger plot of two-dimension confined GeTe film moves to right side in Fig. 2(b), which is attributed to the higher $T_p$ than that of single GeTe film. As we know that the thinner film is, the higher $T_p$ is, which was also found in the phase-change material, like the Sb [13]. The non-phase-change layer W in this confined film divides the GeTe into very thin film with the thickness of 7 nm. Therefore, the confined GeTe film has higher $T_p$. Moreover, the activation energy (curve slope in Fig. 2(b)) of confined GeTe film is larger than that of single film. Such activation energy in confined GeTe film decreases toward higher temperatures, which due to the fragile nature of GeTe PCLs. Compared to the single GeTe film, this change of activation energy in confined film is less, indicating a stronger GeTe PCLs is obtained by using the two-dimension confinement method.

Previously, Henderson discussed the validity of the Kissinger method in non-isothermal crystallization kinetics study and confirmed it cloud be applied when $T_p$ is equal to the temperature at which crystallized faction is 0.63 ($T_{0.63}$) [14]. This confirmation work is also need in chalcogenide PCLs before their crystallization kinetics study. We now first performed the Johnson-Mehl-Avrami (JMA) numerical simulation with the numerous isothermal steps (0.05 K per step) to approximate the non-isothermal heating process. Such JMA numerical simulation was performed many times in previous studies [6,7,15], so the details are not displayed here. Together with the generalized Mauro-Yue-Ellison-Gupta-Allan (g-MYEGA) viscosity model and suitable parameters, we obtained the simulated FDSC traces of confined GeTe film as shown in the upper layer of Fig. 2. The $T_p$ values at different heating rates obtained from the simulated traces are in accord with that obtained from the measured traces, indicating these JMA simulated traces can be used to confirm the validity of the Kissinger method for crystal-

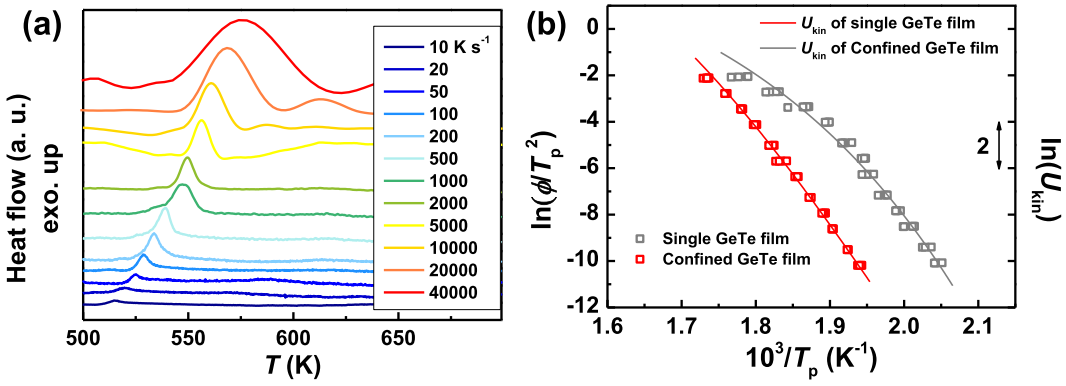


**Fig. 2.** (a) The FDSC traces of $[GeTe(7nm)/W(6nm)]_{20}$ film. (b) The Kissinger plots of this confined GeTe film and single GeTe film. The gray data are the $T_p$ values of GeTe that was published in our previous work [7]. The fitted curves are the temperature dependences of relative crystallization kinetics coefficient $U_{kin}$.

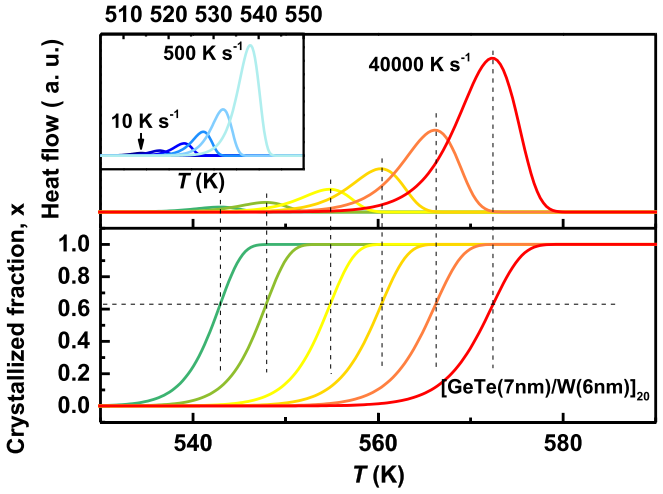


**Fig. 3.** JMA numerical simulated FDSC traces (upper layer) and the corresponding crystallized fraction $x$ (bottom layer) of $[GeTe(7nm)/W(6nm)]_{20}$ film. This region is reached using modeled heating rates from 10 to 40000 K $s^{-1}$. The inset in upper layer shows the simulated FDSC traces of low heating rates (from 10 to 500 K $s^{-1}$). The horizontal dashed line in bottom layer indicates the crystallized fraction of 0.63, and the vertical dashed line indicates the $T_p$ at different heating rate.

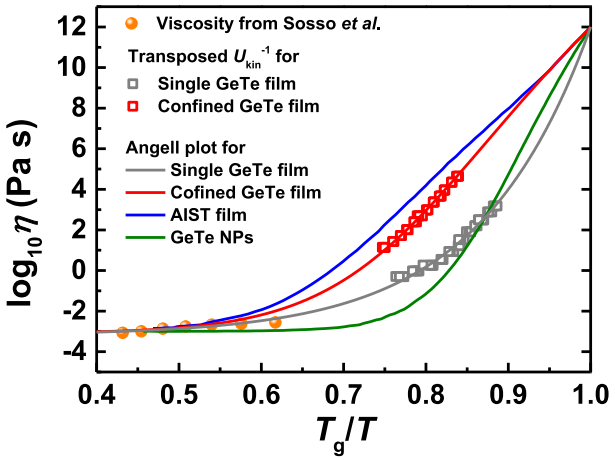


**Fig. 4.** Angell plots of two-dimension confined GeTe and other PCLs. The $T_g$ of GeTe is 432.1 K that has been reported in previous work [7]. The gray and red data are the transposed $U_{kin}^{-1}$ of single GeTe and confined GeTe film, and the corresponding gray and red curves are the Angell plots of GeTe and confined GeTe film by fitting with g-MYEGA viscosity model. The bule and olive curves are the Angell plots of AIST [4] and GeTe nanoparticles (NPs) [9], respectively. The orange spheres indicate the viscosity data of GeTe compound from Sosso *et al.* [18].

lization kinetics study. In order to obtain temperature dependent crystallized fraction ($x$), the simulated FDSC traces were integrated and normalized as exhibited in the bottom layer of Fig. 3. As we see that, there is no any difference between $T_{0.63}$ and $T_p$ could be found in all of the heating rate performed here, indicating the Kissinger method is valid to study the crystallization kinetics and the FSC behavior in this two-dimension confined GeTe PCLs.

According to the Stokes-Einstein relationship of $U_{kin} \propto \eta^{-1}$, which describes the relationship between viscosity $\eta$ and crystallization kinetics coefficient $U_{kin}$, the $U_{kin}$ expression can be described as [16],

$$\log_{10} U_{kin} = C - \log_{10}\eta \tag{2}$$

where $C$ is a constant used to explain the gap between $U_{kin}$ and $\eta^{-1}$. We here used the g-MYEGA viscosity model to describe the temperature dependent viscosity $\eta$ and potential FSC behavior in $[GeTe(7nm)/W(6nm)]_{20}$ film. The g-MYEGA viscosity model is [17],

$$\log_{10}\eta = \log_{10}\eta_\infty + \frac{1}{T[W_1 \exp(-C_1/T) + W_2 \exp(-C_2/T)]} \tag{3}$$

where $\eta_\infty$ is the viscosity at infinite high temperature, $W_1$ and $W_2$ are the weight coefficients to describe the brittle and strong item, and $C_1$ and $C_2$ are the two constraint starting temperature constants corresponding to the two mechanisms of brittleness and strength, respectively. Taking Eq. (3) into Eq. (2), the expression of $U_{kin}$ can be written as,

$$\log_{10} U_{kin} = C - \log_{10}\eta_\infty - \frac{1}{T[W_1 \exp(-C_1/T) + W_2 \exp(-C_2/T)]} \tag{4}$$

By using this expression, we fitted the Kissinger data and obtained the $U_{kin}$ as shown in Fig. 2(a). The fitted parameters of confined GeTe film are, $\eta_\infty = 10^{-3.09}$ Pa s, $W_1 = 0.936$ $K^{-1}$, $W_2 = 2.224 \times 10^{-4}$ $K^{-1}$, $C_1 = 4698.8$ K, $C_2 = 213.6$ K, and $C = 0.22$, with a good fitting degree (R-square is 0.995). Noteworthily, for the single GeTe film that has been studied by the MYEGA viscosity model before, we here performed g-MYEGA model to fitted it again, and the fitted parameters are, $\eta_\infty = 10^{-3.16}$ Pa s, $W_1 = W_2 = 0.0482$ $K^{-1}$, $C_1 = C_2 = 2786.1$ K, and $C$ =-1.2, with R-square is 0.980. Compared to these two sets of fitted parameters, it is found that the value of $\eta_\infty$ is very close because of the GeTe material instinct, but the confined GeTe has larger divergence between $W_1$ and $W_2$ (or $C_1$ and $C_2$), indicating the potential distinct FSC would be exist in this two-dimension confined GeTe PCLs.

Fig. 4 shows the Angell plots of two-dimension confined GeTe and other related PCLs. Together with the g-MYEGA viscosity model (Eq. (3)) and the parameters obtained above, the transposed $U_{kin}^{-1}$ can be fitted very well. As we see that, no FSC behavior presents in single GeTe PCLs with $\eta_\infty$ is $10^{-3.16}$ Pa s and supercooled liquid fragility $m$ is 112. However, a distinct FSC behavior can be found in the confined GeTe PCLs. Orava *et al.* claimed that FSC may be a universal feature in chalcogenide PCLs [4]. However, it does not find in many PCLs, like the GST [6], GeTe [7,19], and Ge-Sb [20]. We have been confirmed it in previous work and found the FSC behavior is not a universal dynamic feature in PCLs [16]. Certainly, the potential FSC can be exist below the $T_g$, which results by the transition of supercooled liquid to solid glass and exhibits a strict Arrhenius behavior. But this is no help to solve the contradiction between thermal stability and crystallization speed in phase-change materials. Therefore, it is important to know what the FSC temperature ($T_{f\text{-}s}$) is. It defines the $T_{f\text{-}s}$ is [21],

$$T_{f-s} = \frac{C_1 - C_2}{\ln W_1 - \ln W_2} \tag{5}$$

Taking the above fitted parameters in to this equation, the $T_{f\text{-}s}$ of two-dimension confined GeTe film can be estimated as 537 K. Thus, the value of $T_g/T_{f\text{-}s}$ is 0.805, which is smaller than that of GeTe NPs (0.91) [9], and larger than that of AIST PCLs (0.72) [4]. Depending on the Angell of plot, we then estimated the fragile index for strong and weak item by the following equation of,

$$m = \left[\frac{d\log_{10}\eta}{d(T_g/T)}\right]_{T=Tg} \tag{6}$$

and

$$m' = \frac{d\log_{10}\eta}{d(T_g/T)}T = Tf - s \tag{7}$$

It yields the fragility $m$ for strong item and fragility $m'$ for weak item are 45 and 89, respectively. Thus, the crossover amplitude ($f$), which is defined as $m/m'$, can be calculated as 2. Above moderate $T_g/T_{f\text{-}s}$ and large $f$ indicate a distinct FSC behavior presents in the confined GeTe PCLs with two-dimension confinement structure.

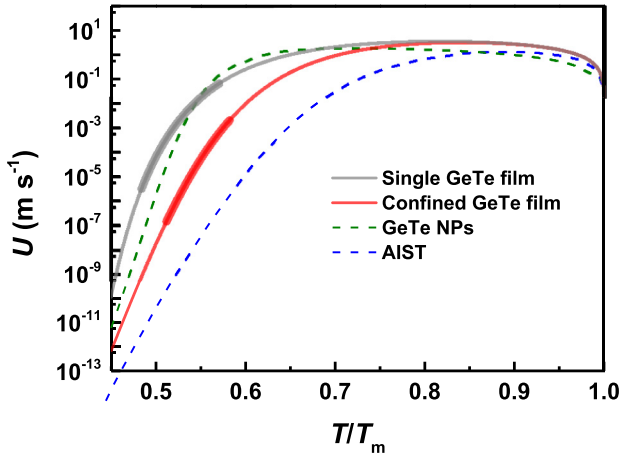


**Fig. 5.** Reduced temperature ($T/T_m$) dependent crystal growth rate ($U$). The thick gray and red curves indicate the FDSC measurement temperature range for single and confined GeTe film, respectively. The blue and olive dashed curves are the temperature dependent crystal growth rates of AIST [4] and GeTe NPs [9].

The temperature dependent crystal growth rate $U$ can be extrapolated by [6],

$$U = U_{kin}[1 - exp(-\Delta G/RT)] \quad (8)$$

where $U_{kin}$ is the absolute crystallization kinetic coefficient (it can be extrapolated together with the absolute $U_{kin}$ value at $T_m$ and the relative $U_{kin}$ obtained from above Kissinger method), $R$ is the gas constant (8.314 J mol$^{-1}$ K$^{-1}$), and $\Delta G$ is the crystallization driving force. It suggests the $\Delta G$ of chalcogenide material (like GeTe studied here) obeys the Thompson and Spaepen equation [22],

$$\Delta G = \frac{\Delta H_m \Delta T}{T_m}\left(\frac{2T}{T_m + T}\right) \quad (9)$$

where $\Delta T$ is the supercooled temperature, $T_m$ and $\Delta H_m$ are the melting temperature and latent heat of fusion, respectively, and they are 1000 K and 17.9 kJ mol$^{-1}$ for GeTe materials. Taking Eq. (9) into Eq. (8), we obtained the temperature dependent $U$ of confined GeTe film as shown in Fig. 5 with the red curve. It was found that, this two-dimension confined GeTe has a large maximum crystal growth rate ($U_{max}$) of 3.2 m s$^{-1}$ at the specific temperature ($T_{max}$) of 0.84 $T_m$ (~840 K). The $U_{max}$ of single GeTe film and GeTe NPs is 3.5 and 1.8 m s$^{-1}$ at the $T_{max}$ is 0.81 and 0.72 $T_m$, respectively. Compared to other GeTe PCLs, it can be concluded that the confinement layer influence on the crystal growth rate is pronounced in applications at lower temperatures but tends to vanish at higher temperatures. This is strongly supported by the results from doped $Sb_xTe$ with capping layer [23]. Apparently, the two-dimension confined GeTe PCLs studied here, has larger $U$ at the temperature where closes to $T_m$ and lower $U$ at the temperature where closes to the $T_g$, which is attributed to the distinct FSC behavior presents in this confined PCLs.

It was found the decrease of cell size is benefit to combine faster switching speed with greater thermal stability in N-GST device [24]. Moreover, by using the same method of FDSC, Orava *et al.* found that the sandwich layers in GST devices could combine inhibition of crystallization at low temperature with acceleration at high temperature [25]. Above findings could be the good explanations for the distinct FSC behavior in $[GeTe(7nm)/W(6nm)]_{20}$ film that has very thin phase-change layer (small size) and non-phase-change layers (like the sandwich layer in device). Two-dimension material is a hot topic in recently, but a single two-dimension layer could not be applied in the phase-change memory. The layer-by-layer technology (multi-layer film), however, becomes a good way to solve the issues in conventional phase-change memory, like the superlattice-like GeSbTe was used to decrease the switching time [26], the interface phase-change material $GeTe/Sb_2Te_3$ was designed to reduce the power consumption [27], the heterostructure $TiTe_2/Sb_2Te_3$ ($TiTe_2$ is non-phase-change layer) was performed to alleviate the data storage noise and drift [28]. Thus, the multi-layer film is certainly beneficial for phase-change performance. We here confirmed two-dimensional confinement could trigger the FSC behavior in PCLs, which is a good explanation to understand many multi-layer films have good thermal stability and fast crystallization speed at the same time. Moreover, we believe the FSC behavior will be further enhanced when the thickness of phase-change layer is continually decreased. Exploring the size dependent crystallization kinetics of two-dimension PCLs must be useful in improving phase-change performance, and this would be present in our future work.

In conclusion, we studied the crystallization kinetics of $[GeTe(7nm)/W(6nm)]_{20}$ PCLs by using the method of FDSC and the viscosity model of g-MYEGA. It was found that, this confined PCLs has a large $U_{max}$ of 3.2 m s$^{-1}$, which is close to that of single GeTe film and larger than that of GeTe NPs, at the $T_{max}$ of 840 K. More importantly, a distinct FSC behavior with a large crossover magnitude $f$ of 2 at the $T_{f\text{-}s}$ of 537 K (a deep supercooled temperature) was found in the confined GeTe PCLs, and the fragility for strong and weak item is 45 and 89, respectively. It confirms that, the two-dimensional confinement could trigger the FSC behavior in the PCLs like GeTe, and make it combines low crystal growth rate near to $T_g$ and fast crystal growth rate close to $T_m$.

## Declaration of Competing Interest

We declare that we have no financial and personal relationships with other people or organizations that can inappropriately influence our work, there is no professional or other personal interest of any nature or kind in any product, service and/or company that could be construed as influencing the position presented in, or the review of, the manuscript entitled.

## Acknowledgment

The Project is supported by the National Natural Science Foundation of China (Grant Nos. 61904091, 61775111, 61775109, 51771216, 51922102, and 62074089), Zhejiang Provincial Natural Science Foundation of China (LR18E010002), the National Key R&D Program of China (2018YFA0703604), the Natural Science Foundation of Ningbo City, China (Grant Nos. 2019A610065, 2019A610059), 3315 Innovation Team in Ningbo City, and sponsored by K. C. Wong Magna Fund in Ningbo University, China.

## References

[1] W. Zhang, R. Mazzarello, M. Wuttig, E. Ma, Nat. Rev. Mater 4 (2019) 150–168.
[2] J.O.A.L. Greer, Handbook of Thermal Analysis and Calorimetry 6 (2018) 685–784.
[3] F. Rao, K. Ding, Y. Zhou, Y. Zheng, M. Xia, S. Lv, Z. Song, S. Feng, I. Ronneberger, R. Mazzarello, W. Zhang, E. Ma, Science 358 (2017) 1423–1427.
[4] J. Orava, D.W. Hewak, A.L. Greer, Adv. Funct. Mater 25 (2015) 4851–4858.
[5] J. Gu, Y. Chen, Q. Zhang, G. Wang, R. Wang, X. Shen, J. Wang, T. Xu, Appl. Phys. Lett 115 (2019) 091903.
[6] J. Orava, A.L. Greer, B. Gholipour, D.W. Hewak, C.E. Smith, Nat. Mater 11 (2012) 279–283.
[7] Y. Chen, G. Wang, L. Song, X. Shen, J. Wang, J. Huo, R. Wang, T. Xu, S. Dai, Q. Nie, Cryst. Growth Des 17 (2017) 3687–3693.
[8] B. Chen, G.H. ten Brink, G. Palasantzas, B.J. Kooi, J. Phys. Chem. C 121 (2017) 8569–8578.
[9] B. Chen, D. de Wal, G.H. Ten Brink, G. Palasantzas, B.J. Kooi, Cryst. Growth Des 18 (2018) 1041–1046.
[10] K. Ito, C.T. Moynihan, C.A. Angell, Nature 398 (1999) 492–495.
[11] L.Liu Faraone, C.Y. Mou, C.W. Yen, S.H. Chen, J. Non-Cryst Solids 121 (2004) 10843.
[12] H.E. Kissinger, Anal. Chem 29 (1957) 1702.

[13] M. Salinga, B. Kersting, I. Ronneberger, V.P. Jonnalagadda, X.T. Vu, M. Le Gallo, I. Giannopoulos, O. Cojocaru-Miredin, R. Mazzarello, A. Sebastian, Nat. Mater 17 (2018) 681–685.
[14] D.W. Henderson, J. Non-Cryst Solids 30 (1979) 301–315.
[15] Y. Chen, H. Pan, S. Mu, G. Wang, R. Wang, X. Shen, J. Wang, S. Dai, T. Xu, Acta Mater 164 (2019) 473–480.
[16] Y. Chen, J. Gu, Q. Zhang, Y. Mao, G. Wang, R. Wang, X. Shen, J.-Q. Wang, T. Xu, Phys. Rev. Mater (2020) 4.
[17] C. Zhang, L. Hu, Y. Yue, J.C. Mauro, J. Chem. Phys 133 (2010) 014508.
[18] G.C. Sosso, J. Behler, M. Bernasconi, Phys. Status Solidi 249 (2012) 1880–1885.
[19] H. Weber, J. Orava, I. Kaban, J. Pries, A.L. Greer, Phys. Rev. Mater (2018) 2.
[20] B. Chen, J. Momand, P.A. Vermeulen, B.J. Kooi, Cryst. Growth Des 16 (2015) 242–248.
[21] C. Zhou, L. Hu, Q. Sun, H. Zheng, C. Zhang, Y. Yue, J. Chem. Phys 142 (2015) 064508.
[22] C.V. Thompson, F. Spaepen, Acta Metall 27 (1979) 1855–1859.
[23] R. Pandian, B.J. Kooi, J.T.M. De Hosson, A. Pauza, J. Appl. Phys 100 (2006) 123511.
[24] W. Wang, D. Loke, L. Shi, R. Zhao, H. Yang, L.T. Law, L.T. Ng, K.G. Lim, Y.C. Yeo, T.C. Chong, A.L. Lacaita, Sci. Rep 2 (2012) 360.
[25] J. Orava, A.L. Greer, B. Gholipour, D.W. Hewak, C.E. Smith, Appl. Phys. Lett 101 (2012) 091906.
[26] D. Loke, L. Shi, W. Wang, R. Zhao, H. Yang, L.T. Ng, K.G. Lim, T.C. Chong, Y.C. Yeo, Nanotechnology 22 (2011) 254019.
[27] X.-B. Li, N.-K. Chen, X.-P. Wang, H.-B. Sun, Adv. Funct. Mater 28 (2018) 1803380.
[28] K.Y. Ding, J.J. Wang, Y.X. Zhou, H. Tian, L. Lu, R. Mazzarello, C.L. Jia, W. Zhang, F. Rao, E. Ma, Science 366 (2019) 210.